Interdomain Interactions within the Two-Component Heme-Based Sensor DevS from *Mycobacterium tuberculosis*†

Erik T. Yukl,‡ Alexandra Ioanoviciu,§ Paul R. Ortiz de Montellano,§ and Pierre Moënne-Loccoz*,‡

Department of Environmental & Biomolecular Systems, OGI School of Science and Engineering, Oregon Health & Science University, 20,000 NW Walker Road, Beaverton, Oregon 97006-8921, and Department of Pharmaceutical Chemistry, University of California, 600 16th Street, San Francisco, California 94158-2517

Received May 7, 2007; Revised Manuscript Received June 13, 2007

ABSTRACT: DevS is the sensor of the DevS-DevR two-component regulatory system of *Mycobacterium tuberculosis*. This system is thought to be responsible for initiating entrance of this bacterium into the nonreplicating persistent state in response to NO and anaerobiosis. DevS is modular in nature and consists of two N-terminal GAF domains and C-terminal histidine kinase and ATPase domains. The first GAF domain (GAF A) binds heme, and this cofactor is thought to be responsible for sensing environmental stimuli, but the function of the second GAF domain (GAF B) is unknown. Here we report the RR characterization of full-length DevS (FL DevS) as well as truncated proteins consisting of the single GAF A domain (GAF A DevS) and both GAF domains (GAF A/B) in both oxidation states and bound to the exogenous ligands CO, NO, and O_2. The results indicate that the GAF B domain increases the specificity with which the distal heme pocket of the GAF A domain interacts with CO and NO as opposed to O_2. Specifically, while two comparable populations of CO and NO adducts are observed in GAF A DevS, only one of these two conformers is present in significant concentration in the GAF A/B and FL DevS proteins. In contrast, hydrogen bond interactions at the bound oxygen in the oxy complexes are conserved in all DevS constructs. The comparison of the data obtained with the O_2 complexes with those of the CO and NO complexes suggests a model for ligand discrimination which relies on a specific hydrogen-bonding network with bound O_2. It also suggests that interactions between the two GAF domains are responsible for transduction of structural changes at the heme domain that accompany ligand binding/dissociation to modulate activity at the kinase domain.

Mycobacterium tuberculosis (MTB)[1] is a remarkably successful pathogen thought to have latently infected 2 billion people worldwide (*1*). Part of the reason for this organism's success is its ability to exist within the host in a state known as "nonreplicating persistence" (NRP) for extended periods, reactivating at any point to cause clinical disease. Current chemotherapies act rapidly on growing bacteria, but subpopulations in the dormant state are phenotypically resistant (*2*). For this reason, 6 months is often required to cure the disease, making patient compliance difficult. Thus, a detailed understanding of NRP and the signals that initiate it are critical for improvements in the treatment of TB.

NRP can be modeled *in vitro* by the gradual depletion of oxygen from MTB cultures (*3*). Expression profiles of such cultures indicate that 47 MTB genes are upregulated in response to hypoxic conditions (*4*). Included in this set is α-crystallin, a heat-shock protein likely involved in the stabilization of essential proteins and cell structures during extended quiescence (*5*). A separate study found that a common set of 48 genes was induced in response to both hypoxia and exposure to nontoxic concentrations of NO (*6*). Further, O_2 was shown to competitively inhibit NO-mediated induction of the so-called "dormancy regulon". These observations strongly suggest that one sensor is responsible for detecting both signals and initiating the expression profile responsible for NRP *in vitro*. Such conditions are likely to prevail *in vivo* where the immune response traps the bacteria in microaerobic or anaerobic granulomas (*7*) and where the host expression of endothelial and inducible nitric oxide synthases (eNOS and iNOS) is enhanced in infected tissues (*8*).

It is now believed that the regulatory system DevR/S/T (also known as DosR/S/T), originally identified by the preferential expression of DevR and DevS in virulent over avirulent MTB strains (*9*), is responsible for mediating the response of MTB to hypoxia and NO. DevR is a response regulator of the LuxR family (*9*). DevS, and its paralog DevT, are histidine protein kinases (HPK) capable of

† This work was supported by Grants GM74785 (P.M.-L.) and PO1 GM56531 and AI074824 (P.R.O.M.) from the National Institutes of Health.

* To whom correspondence should be addressed. Tel: 503-748-1673. Fax: 503-748-1464. E-mail: ploccoz@ebs.ogi.edu.

‡ Oregon Health & Science University.

§ University of California.

[1] Abbreviations: MTB, *Mycobacterium tuberculosis*; NRP, nonreplicating persistence; GAF domain, protein domain conserved in cyclic GMP-specific and stimulated phophodiesterases, adenylate cyclases, and *Escherichia coli* formate hydrogenlyase transcriptional activator (Pfam accession number PF01590); GAF A and GAF B, first and second N-terminal GAF domains of DevS; FL DevS, full-length DevS; HPK, histidine protein kinases; HisKA, histidine kinase phosphor-acceptor domain, HATPase, histidine kinase-like ATPase domain; wt, wild-type; IPTG, isopropyl-β-D-thiogalactopyranoside; RR, resonance Raman.

10.1021/bi7008695 CCC: $37.00
Published on Web 08/03/2007

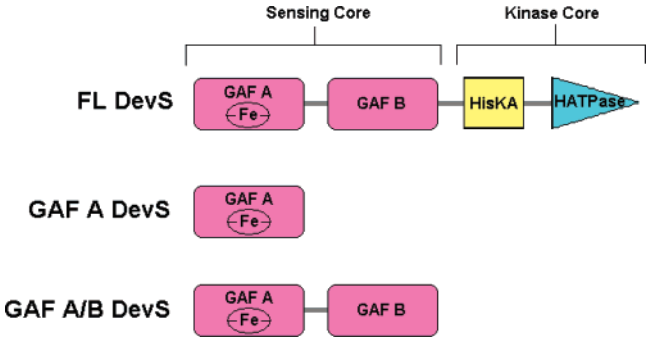

FIGURE 1: Domain organization of wild-type and truncated *M. tuberculosis* DevS. Domain nomenclatures, symbols, and protein organizations are according to the simple modular architecture research tool (SMART) from the European Molecular Biology Laboratory (*37*).

autophosphorylation at a conserved histidine residue and subsequent transfer of the phosphate group to an aspartate residue of DevR (*10*). Phosphorylation of DevR enhances its affinity for palindromic DNA sequences that precede nearly every MTB gene upregulated in the hypoxic response (*10*). MTB mutants Δ*dosR* (*6*) and Δ*dosS:*Δ*dosT* (*10*) are unable to activate gene expression in response to hypoxia, making the DevR/S/T system an attractive target for treatment of persistent MTB infection.

Both DevS and DevT are modular in nature and consist of an N-terminal sensing core composed of two tandem GAF domains and a C-terminal kinase core with a HisKA (histidine kinase phosphor-acceptor) domain where autophosphorylation occurs and a HATPase (histidine kinase-like ATPase) domain responsible for binding ATP (*11*) (Figure 1). The first GAF domain (GAF A) of DevS was recently shown to bind heme (*11*, *12*). Because CN^- prevents induction of the dormancy regulon by NO and hypoxia (*6*), and because hemes often present high affinities for NO and O_2, the GAF A domain is likely to be responsible for diatomic gas sensing in DevS. This led to the proposal put forward by Sardiwal et al. (*11*) that the kinase activity of DevS is optimal when the heme is in the deoxy state, signaling hypoxia. This activity is strongly inhibited by the binding of O_2 to the heme, but only very slightly inhibited by the binding of NO, leaving the kinase domain deregulated. However, the questions of how the protein differentiates between NO and O_2 and how these signals are communicated to the histidine kinase domain remain unanswered.

Recently, we reported the resonance Raman (RR) characterization (RR) of a truncated wild type (wt) DevS containing only the N-terminal GAF domain (GAF A DevS) as well as an H149A variant of this construct and the initial characterization of the full-length DevS (*12*). The results indicated that His 149 is the proximal ligand to the heme iron. We also observed that the wt GAF domain bound CO in two distinct conformations whereas the full-length protein appeared to support only one of these conformations. Here we further investigate this phenomenon with the RR characterization of full-length wt-DevS (FL DevS), GAF A DevS, and a new construct composed of both GAF domains (GAF A/B DevS) (Figure 1). All constructs in both oxidation states, as well as bound to the exogenous ligands CO, NO, and O_2, were investigated. The results indicate that interaction between the GAF A and GAF B domains enhances the specificity of the interaction between exogenous ligands and the heme distal pocket, allowing the protein to distinguish between O_2 and other diatomics such as NO and CO. As such, these interactions may represent a means of signal transduction linking the state of the heme to the activity of the kinase domain. Within the context of signal transduction, the GAF B domain is proposed to be an actuator domain that couples the sensory and the kinase functions in DevS. Possible mechanisms for differentiating between exogenous ligands are also discussed.

MATERIALS AND METHODS

Cloning, Protein Expression, and Purification. Cloning, expression, and purification of the three DevS proteins were performed as described in ref 12. Briefly, the desired DNA sequence was PCR amplified from the plasmid coding for the entire DevS gene previously obtained in the TOPO TA experiment. The PCR product was then ligated into pET23a+. The DevS constructs were co-overexpressed with the GroEL/ES complex in BL21DE3 cells. The recombinant protein was purified using nickel affinity chromatography. DevS379 includes the first 379 amino acids of DevS, and it contains the two GAF domains of DevS. The reverse primer used for the cloning of DevS379 was GGTGAAGCTTCTATT-AGCGCATCCGACGTTGCGAAGTGGC, and the same forward primer was employed as for the full-length DevS and DevS624 (first 642 bp coding for the Gaf A domain).

Electronic Absorption and Resonance Raman Spectroscopy. Typical enzyme concentrations used were ∼100−300 μM. Biomax-10 ultrafiltration devices (Millipore) were used for buffer exchange and for concentrating the proteins. A 50 mM potassium phosphate buffer at pH 7.5 with 200 mM NaCl was used for all protein samples. Reduction to the ferrous state was achieved by adding microliter aliquots of concentrated sodium dithionite solution (35−50 mM) to an argon-purged sample in the Raman capillary cell and was monitored by UV−vis spectroscopy directly in the capillary using a Cary 50 spectrometer. ^{12}CO (Airgas) and ^{13}CO (99% ^{13}C; ICON Stable Isotopes) adducts were obtained by injecting CO through a septum-sealed capillary containing argon-purged, reduced protein (∼20 μL). O_2 (Airgas), $^{18}O_2$ (99% ^{18}O; ICON Stable Isotopes), NO (Aldrich), $^{15}N^{16}O$ (99% ^{15}N; ICON Stable Isotopes), and $^{15}N^{18}O$ (98% ^{15}N and 95%^{18}O; Aldrich) adducts were generated using the same procedure after excess dithionite was removed from the reduced sample with desalting spin columns (Zeba 0.5 mL; Pierce). These procedures were performed in a glovebox with a controlled atmosphere of less than 1 ppm O_2 (Omni-Lab System; Vacuum Atmospheres Co.).

RR spectra were obtained using a custom McPherson 2061/207 spectrograph (0.67 m with variable gratings) equipped with a Princeton Instruments liquid N_2-cooled CCD detector (LN-1100PB). Kaiser Optical supernotch filters were used to attenuate Raleigh scattering. A krypton laser (Innova 302, Coherent) and a He/Cd laser (Liconix 4240NB) were used for 413 and 442 nm excitations, respectively. Spectra were collected in a 90° scattering geometry at room temperature on samples mounted on a reciprocating translation stage. Frequencies were calibrated relative to indene and CCl_4 and are accurate to ±1 cm^{-1}. CCl_4 was also used to check the polarization conditions. The integrity of the RR samples,

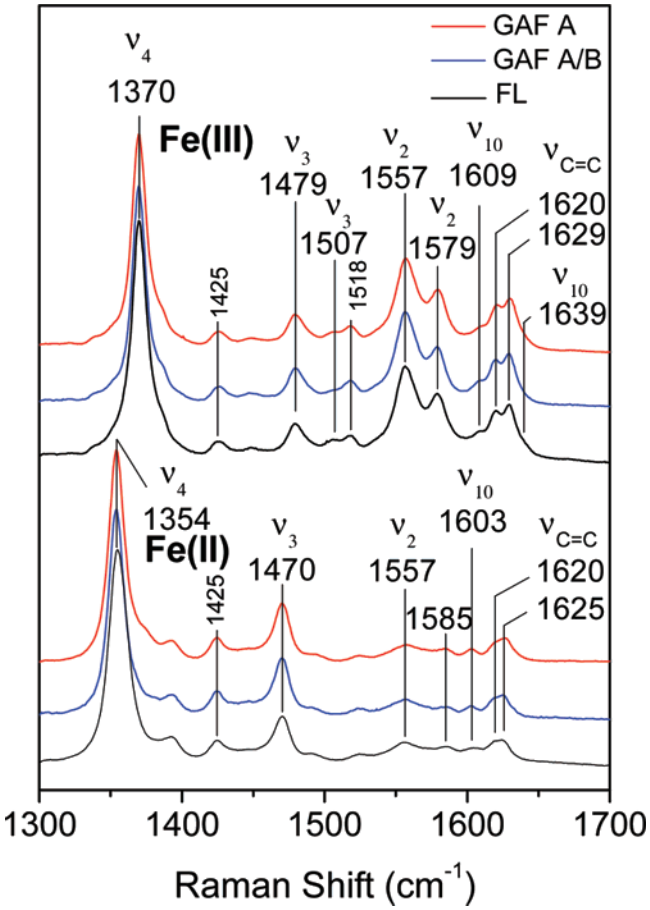

FIGURE 2: High-frequency RR spectra of ferric (top traces) and ferrous (bottom traces) GAF A DevS (red), GAF A/B DevS (blue), and FL DevS (black) at room temperature (λ_{exc} = 413 nm, 5 mW).

before and after laser illumination, was confirmed by direct monitoring of their UV−vis spectra in the Raman capillaries.

RESULTS

Overall Heme Binding Pocket Structure of DevS Constructs, FL DevS, GAF A DevS, and GAF A/B DevS. The near identity of the electronic absorption (Figure S1, Supporting Information) and high-frequency RR (Figure 2) spectra of the ferric and ferrous states of all three DevS constructs studied suggests a conserved heme pocket structure and coordination. The coordination number, spin state, and oxidation state of the heme iron of the DevS constructs are correlated to the frequencies of the ν_4, ν_3, ν_2, and ν_{10} modes in the high-frequency region of the RR spectra obtained with Soret excitation (*13*). Other porphyrin vibrations routinely observed in RR spectra of hemoproteins (e.g., ν_{28} at 1425 cm^{-1} and ν_{38} at 1518 cm^{-1} in Figure 2) are not readily correlated to structural parameters. At room temperature and neutral pH, ferric DevS constructs exhibit ν_4, ν_3, ν_2, and ν_{10} at 1370, 1479, 1557, and 1609 cm^{-1}, respectively. The frequencies of these bands are characteristic of a 6-coordinate high-spin (6cHS) heme (Figure 2). A minor 6-coordinate low-spin (6cLS) species is evidenced by a shoulder at 1507 cm^{-1} in the range of ν_3 modes. The intense high-spin charge-transfer marker band at 630 nm in the UV−vis spectrum (Figure S1) and the dominance of high-spin marker bands in the RR spectra (Figure 2) support the assignment of the high-spin state as the major conformer in the ferric proteins. Upon reduction with dithionite, the ferrous DevS constructs adopt a pure 5-coordinate high-spin (5cHS) configuration with ν_4, ν_3, ν_2, and ν_{10} at 1354, 1470, 1557, and 1603 cm^{-1}, respectively (Figure 2). Using a 442 nm excitation wavelength on the reduced protein allows for the observation of a ν(Fe−N_{His}) at 214 cm^{-1} in all constructs (Figure 3). This band arises from proximal ligation of the heme iron by His 149 (*12*).

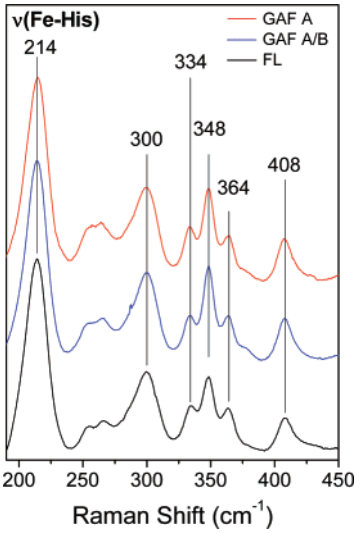

FIGURE 3: Low-frequency RR spectra of ferrous GAF A DevS (red), GAF A/B DevS (blue), and FL DevS (black) at room temperature (λ_{exc} = 442 nm, 15 mW).

Table 1: UV−Vis Spectroscopic Data for Wt DevS Constructs

heme state	Soret band (nm)	visible bands (nm)
Fe(III)	406	500, 630
Fe(II)	428	562
Fe(II)−CO	422	570, 540
Fe(II)−NO	419	577, 547
Fe(II)−O_2	414	578, 543

Addition of CO, NO, or O_2 to dithionite-reduced DevS constructs results in the formation of stable, 6-coordinate adducts in all cases as determined by the position of Soret absorbance in the UV−vis spectra (Table 1). The near identity of the high-frequency RR spectra of the truncated and full-length DevS constructs bound to these ligands reinforces results seen in the ferric and ferrous states, indicating that truncation does not significantly perturb the structure or coordination of the bound heme (data not shown).

Vibrations of the heme peripheral groups can also be indicative of the heme conformation. These modes are identified in DevS based upon analogy to assigned vibrations in myoglobin (*14*). Two vinyl stretching modes, $\nu_{(C=C)}$, are observed at 1620 and 1629 cm^{-1} in the ferric states and at 1620 and 1625 cm^{-1} in the ferrous states of all DevS constructs (Figure 2). Moreover, the 300−450 cm^{-1} spectral region of the RR spectra of all three ferrous DevS constructs clearly demonstrates that δ(CCC) deformation modes from the vinyl and propionate groups are not perturbed by truncations of the GAF B and/or the kinase domains (Figure 3). Analysis of this spectral region in the RR spectra of the CO, NO, and O_2 adducts of DevS illustrates a similar phenomenon. Two bands, assigned to δ(CCC) of heme propionate groups, appear at nearly identical frequencies for the truncated and full-length DevS bound to CO (379 and

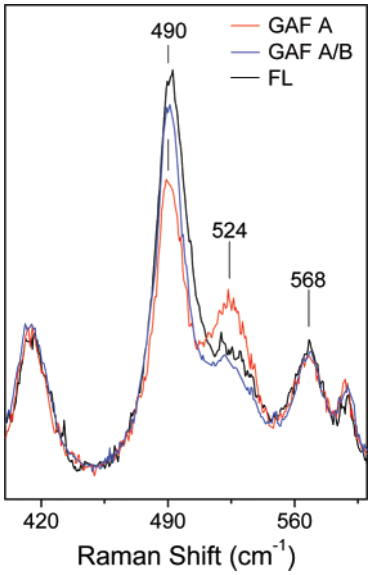

FIGURE 4: Low-frequency RR spectra of GAF A DevS-^{12}CO (red), GAF A/B DevS-^{12}CO (blue), and FL DevS-^{12}CO (black) at room temperature (λ_{exc} = 413 nm, <0.5 mW).

387 cm^{-1}; Figure S2, Supporting Information), NO (378 and 385 cm^{-1}; Figure S4), and O_2 (375 and 385 cm^{-1}; Figure 8). These observations illustrate how the heme anchoring by peripheral groups is conserved in truncated and full-length DevS constructs, further supporting our conclusion that truncation has no major effect on heme binding within the GAF A domain of DevS. The similar frequencies of the heme propionate group vibrations for DevS bound to all three exogenous ligands suggest that hydrogen bonding around the heme propionate groups is similar in all cases, making a role for these peripheral groups in ligand discrimination unlikely.

Carbonyl Complexes. Despite the overall similarity of the CO complexes in truncated and full-length DevS, analysis of isotope-sensitive modes illustrates important differences in the organization of the distal pockets of DevS constructs. We have previously reported the observation of two CO conformers in GAF A DevS (*12*). Briefly, the low-frequency RR spectra of GAF A DevS-CO show isotope-sensitive bands at 490 and 524 cm^{-1} that downshift by 3 and 4 cm^{-1}, respectively, upon ^{13}CO substitution (Figure S2). Based on the isotope shifts, these bands were assigned to two distinct ν(Fe−CO) modes (Figure 4 and S2). Corresponding ν(C−O) bands appear at 1936 and 1971 cm^{-1} with ^{12}CO/^{13}CO shifts of −43 and −44 cm^{-1}, respectively (Figure 5A,B). The observed frequencies are characteristic of heme−carbonyl complexes with a neutral histidine coordinating *trans* to the CO group (*15*). The degree of back-bonding as determined from the correlation of ν(C−O) and ν(Fe−CO) vibrational frequencies suggests that one of the CO conformers (ν(Fe−CO) = 524 cm^{-1}; ν(C−O) = 1936 cm^{-1}) is engaged in electrostatic and/or hydrogen bond interaction(s) within the distal pocket while the other conformer (ν(Fe−CO) = 490 cm^{-1}; ν(C−O) = 1971 cm^{-1}) is in a hydrophobic environment (Figure S3, Supporting Information). The proximity of these correlation points to those of the V68N variant of myoglobin, which has an additional polar group in the distal pocket (ν(Fe−CO) = 526 cm^{-1}; ν(C−O) = 1922 cm^{-1}) (*16*, *17*) and the H64L variant of myoglobin with no polar distal group (ν(Fe−CO) = 490 cm^{-1}; ν(C−O) = 1965 cm^{-1}) (*16*, *18*), respectively, supports such a conclusion (Figure S3). RR spectra acquired for GAF A DevS in this study confirm the previous analysis and also identify a δ(Fe−C−O) mode at 568 cm^{-1} which downshifts 12 cm^{-1} upon substitution with ^{13}CO (Figure S2).

In GAF A/B DevS, the relative populations of the heme-CO conformers have changed significantly from those observed in GAF A DevS to favor the conformation lacking the distal interaction (Figures 4 and 5C,D). Control experiments at minimal laser power confirm that photolysis of heme-carbonyl complexes does not play a role in the differences observed between DevS constructs (data not shown). Peak fitting analysis comparing GAF A DevS and GAF A/B DevS indicates that introduction of the GAF B domain alone is sufficient to decrease the intensity of the ν(C−O) at 1936 cm^{-1} by more than half (Figure 5). The low- and high-frequency RR spectra of FL DevS bound to CO are similar to those of GAF A/B DevS-CO (Figures 4 and 5E,F). Although the inclusion of the kinase and ATPase domains may lead to further reduction in the population of the CO conformer with the distal interactions, the effect is too subtle to be reliably observed in the RR data (Figure 5). Thus, it seems that the conformational flexibility that allows GAF A DevS to stabilize two CO conformers in the distal pocket is restricted upon the introduction of the GAF B domain. This suggests an interaction between GAF A and GAF B that increases the specificity of the interaction between bound CO and the distal heme pocket.

Nitrosyl Complexes. The ν(N−O) modes of heme−nitrosyl complexes are also sensitive to the electrostatics of the distal environment (*19*). These modes reside in a spectral region that is dominated by intense porphyrin ring modes, making their assignment from primary spectra extremely difficult. Difference spectra of ^{14}N^{16}O and ^{15}N^{18}O DevS adducts are therefore used for their identification. Analogous to the carbonyl complex data, the ^{14}N^{16}O−^{15}N^{18}O difference spectrum for the GAF A DevS nitrosyl complex (Figure 6A) shows two isotope sensitive bands at 1638 and 1604 cm^{-1} that downshift approximately 72 and 73 cm^{-1}, respectively, upon ^{15}N^{18}O substitution. These shifts are in good agreement with the calculated ^{14}N^{16}O−^{15}N^{18}O shift values of −73 and −72 cm^{-1} for these two bands, respectively. Reproducible spectral features at 1627 and 1577 cm^{-1} are attributed to vibrational mixing between the ν(^{15}N−^{18}O) and the vinyl stretch and the ν_2 mode, respectively, as has been observed in other systems (*19*). A positive feature at 1502 cm^{-1} is systematically observed in the ^{14}N^{16}O−^{15}N^{18}O difference spectrum, but it is absent from the ^{14}N^{16}O−^{15}N^{16}O difference spectrum (Figure 6 and S5, Supporting Information). The origin of this signal is unclear; it may reflect differences in intensity borrowing and combination bands involving ν(Fe−NO) and/or δ(Fe−N−O). Despite these complications, the assignment of two distinct ν(^{14}N−^{16}O) modes can be made with confidence given the excellent agreement between experimental and calculated shift values and the close correlation between ν(N−O) and ν(C−O) modes as has been observed with heme proteins sharing the same proximal ligation (Figure 7) (*20*). Again, the difference between the nitrosyl conformers can be attributed to the presence of a hydrogen bond in one conformer, giving rise to the low-frequency N−O stretch through enhanced back-bonding. These spectra also show a decrease in the relative intensity of the low frequency ν(N−O) upon addition of the second

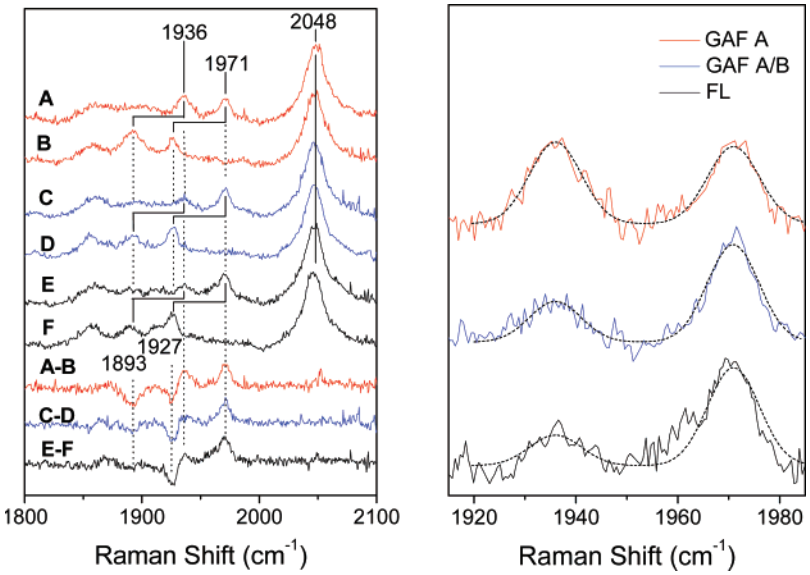

FIGURE 5: Left panel: High-frequency RR spectra of GAF A DevS-^{12}CO (A, red), GAF A DevS-^{13}CO (B, red), GAF A/B DevS-^{12}CO (C, blue), GAF A/B DevS-^{13}CO (D, blue), FL DevS-^{12}CO (E, black), and FL DevS-^{13}CO (F, black). Right panel: Peak fitting analysis of the ν(C−O) modes in GAF A DevS-^{12}CO (red), GAF A/B DevS-^{12}CO (blue), and FL DevS-^{12}CO (black). Peak positions (1936 and 1971 cm^{-1}) and peak widths (12 cm^{-1}) determined from the analysis of GAF A DevS-CO were fixed to fit the data of GAF A/B DevS-CO and FL DevS-CO.

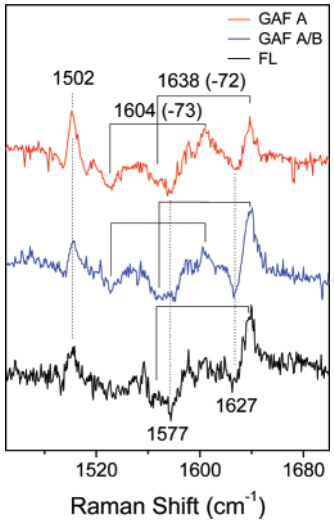

FIGURE 6: High-frequency RR spectra of ^{14}N^{16}O−^{15}N^{18}O difference spectra for the ferrous-nitrosyl adducts of GAF A DevS (red), GAF A/B DevS (blue), and FL DevS (black) at room temperature (λ_{exc} = 413 nm, 0.5 mW).

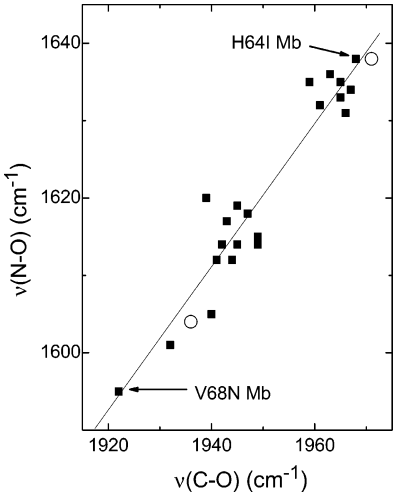

FIGURE 7: ν(N−O) versus ν(C−O) plots of heme protein−NO and −CO complexes. Data points for wt DevS constructs (○) are compared with values for wt and distal mutants of myoglobin (*20*) (■).

GAF domain (Figure 6). The spectrum of the full-length protein is similar to that of GAF A/B DevS, potentially showing even greater attenuation of the hydrogen-bonded NO conformer (Figure 6). This observation would again seem to indicate that GAF B interacts with GAF A, leading to a more specific interaction between bound NO and the distal heme pocket.

In contrast to the ν(N−O) mode, the ν(Fe−NO)s of heme−nitrosyl complexes are not particularly sensitive to the electrostatic environment of the bound NO (*19*). Figure S6 (Supporting Information) shows low-frequency spectra of the ^{14}N^{16}O and ^{15}N^{16}O adducts of FL DevS as well as ^{14}N^{16}O−^{15}N^{16}O difference spectra of all DevS constructs. In each case, an isotope sensitive band is identified at 561 cm^{-1} and is assigned to a ν(Fe−NO) mode. Although minor differences in position and/or bandwidth of ν(Fe−NO) in full-length and truncated DevS constructs may exist, the low intensity of these vibrations and their known coupling (*21*) preclude their reliable observation and correlation to structural perturbation (data not shown).

Oxy Complexes. Low-frequency RR spectra of the $^{16}O_2$ and $^{18}O_2$ complexes of DevS constructs and their difference spectra are shown in Figure 8. In contrast to the trends seen for the DevS adducts of other exogenous ligands, there seems to be no difference in how the DevS constructs bind oxygen, based on their $^{16}O_2$−$^{18}O_2$ difference spectra (Figure 8). Each construct presents a ν(Fe−O_2) at 563 cm^{-1} that downshifts 22 cm^{-1} upon $^{18}O_2$ substitution, a value that is in good agreement with the calculated shift of −25 cm^{-1}, assuming a diatomic Fe−O oscillator. Although the presence of multiple Fe−O_2 stretching modes cannot be ruled out, the conserved width and shape of the derivative feature in the difference spectra of all constructs suggest that, if multiple conformations of O_2 are present, their relative populations remain unchanged in truncated and full-length proteins

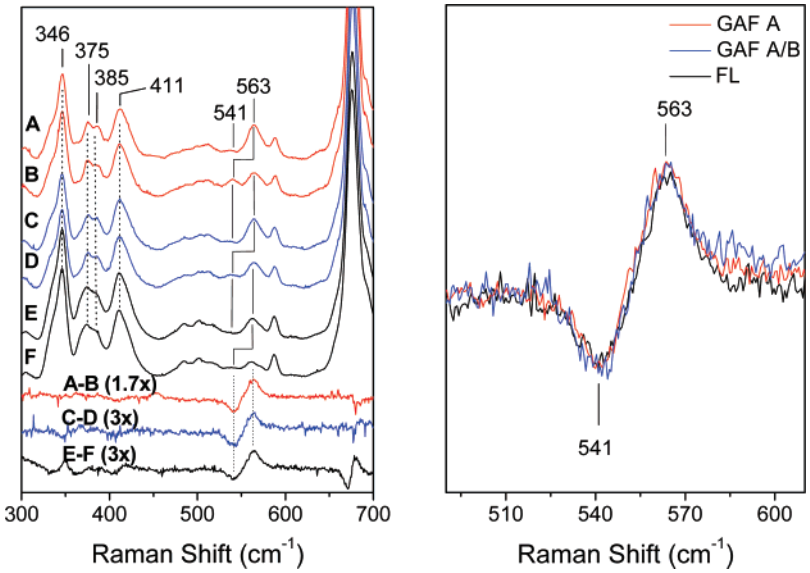

FIGURE 8: Left panel: Low-frequency RR spectra of GAF A DevS-$^{16}O_2$ (A, red), GAF A DevS-$^{18}O_2$ (B, red), GAF A/B DevS-$^{16}O_2$ (C, blue), GAF A/B DevS-$^{18}O_2$ (D, blue), FL DevS-$^{16}O_2$ (E, black), and FL DevS-$^{18}O_2$ (F, black). Right panel: Overlay of $^{16}O_2-^{18}O_2$ difference spectra of GAF A DevS (red), GAF A/B DevS (blue), and FL DevS (black) oxygen adducts (λ_{exc} = 413 nm, 1.0 mW).

(Figure 8). Although this mode is not as sensitive a probe for the distal environment as the ν(N−O) or ν(C−O) modes, the lack of any observable difference between the oxy complexes of different constructs strongly suggests that, unlike CO and NO, O_2 binds to DevS in the same conformation(s) regardless of the presence or absence of the GAF B and kinase domains.

The ν(Fe−O_2) frequencies observed in the different DevS constructs are at the lower end of heme-O_2 adducts with neutral histidine trans ligand (*22*) and are suggestive of strong distal hydrogen bonding to the proximal oxygen atom of the bound O_2 as in heme oxygenases (ν(Fe−O_2) = 565 cm^{-1}) (*23*, *24*) and hemoglobins from *Mycobacterium* (ν(Fe−O_2) = 560 cm^{-1}) (*25*) and *Paramecium* (ν(Fe−O_2) = 563 cm^{-1}) (*26*). To test this hypothesis, the D_2O sensitivity of the ν-(Fe−O_2) mode in DevS was also examined. The H_2O − D_2O difference spectra of the $^{16}O_2$ adducts of all DevS constructs illustrate the effect of H/D exchange, showing maxima and minima at 563 and 575 cm^{-1}, respectively (Figure 9). The effect of H/D exchange can also be examined by comparing the $^{16}O_2-^{18}O_2$ difference spectra in H_2O and D_2O. Indeed, the derivative signal in the $^{16}O_2-^{18}O_2$ difference spectra of GAF A DevS and FL DevS in D_2O is upshifted 4 to 5 cm^{-1} relative to that in H_2O (Figure S7, Supporting Information). The discrepancy in shift values obtained by each method suggests Fermi coupling between the ν(Fe−O_2) and porphyrin ring modes. Despite this added complexity, both methods show that H/D exchange perturbs the ν(Fe−O_2) and further support the presence of hydrogen bonding from a distal residue to bound O_2 in truncated and full-length DevS constructs.

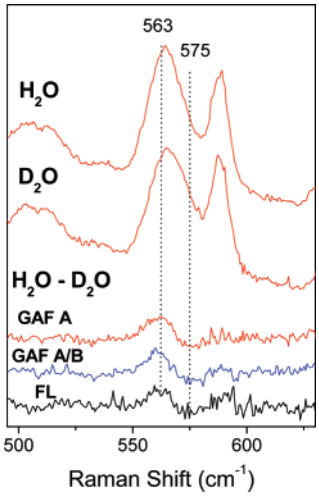

FIGURE 9: Low-frequency RR spectra of GAF A DevS-$^{16}O_2$ in H_2O buffer and D_2O buffer (top two traces, red) and H_2O-D_2O difference of GAF A DevS-$^{16}O_2$ (red), GAF A/B DevS-$^{16}O_2$ (blue), and FL DevS (black) (λ_{exc} = 413 nm, 1.0 mW).

DISCUSSION

Comparison of the RR spectra of full-length and truncated constructs of DevS allows for the investigation of interdomain interactions in terms of their impact on the heme environment. The essentially identical UV−vis spectra (Figure S1), porphyrin core marker RR frequencies (Figure 2), propionate and vinyl peripheral group vibrations (Figures 2, 3, 8, S2, and S4, Supporting Information), and Fe-His stretching vibrations (Figure 3) in all DevS constructs demonstrate that truncation of the GAF B and kinase domains does not alter the proximal environment or the anchoring of the heme group in the GAF A domain. However, analysis of the isotope sensitive modes of the CO (Figures 4 and 5) and NO (Figure 6) adducts of these constructs shows that the distal environment is impacted by the presence of the GAF B domain. Specifically, the presence of this domain causes a significant perturbation in the relative populations of the two CO and NO conformers present in GAF A DevS, causing a preference for the conformation lacking a strong hydrogen bond. Therefore, interactions between the two GAF domains of DevS limit the conformational flexibility of the heme distal pocket and destabilize the hydrogen-bonded conformers of the CO and NO heme adducts.

Although the direct observation of interdomain interactions by RR spectroscopy is unusual, similar observations have been made when comparing truncations of *Rhizobium*

Table 2: Resonance Raman Frequencies (cm^{-1}) of O_2, NO, and CO Bound to Ferrous Heme Sensor Proteins

protein	ν(Fe−O_2)	ν(Fe−NO)	ν(N−O)	ν(Fe−CO)	ν(C−O)
FL DevS[a]	563	561	1638, 1604[f]	490, 524[f]	1971, 1936[f]
*Bs*HemAT[b]	560	545	1636	494	1964
*Ec*DosH[c]	562	563	1632/1576	487	1969
*Rm*FixL[d]	571	525/558	1676/1664[g]	502	1956
SW Mb[e]	570	560	1613	512	1944

[a] This work. [b] References *29, 33*. [c] Reference *30*. [d] References *27, 28, 34*. [e] References *19, 35, 36*. [f]Observed in the truncated heme domain (DevS GAF A). [g] Observed only in the truncated heme domain at low temperature (−45 °C).

meliloti FixL, another modular heme-based sensor kinase (*27*). In this case, two 5-coordinate ν(N−O) modes were detected in the low-temperature RR spectrum of the isolated heme domain of FixL-NO. In the construct that included the kinase domain, only one of these modes was observed. This difference was interpreted as arising from contact between the kinase and heme domains, which caused a more specific interaction between the bound NO and the heme distal pocket. The kinase domain of FixL also modulates interactions between the heme distal pocket and bound CO. Although only one ν(C−O) mode was detected in both truncated FixL-CO and functional kinase FixL-CO, its frequency was found to be 6 cm^{-1} higher in the functional kinase than in the truncated heme domain (*28*). Thus, interaction between the kinase and heme domains of *Rm*FixL modulates the interaction of the distal pocket with both CO and NO ligands.

The nature of the change that occurs in the distal pocket of FixL in the presence of the kinase domain remains uncertain. Miyatake et al. suggest that the relatively small shift in the ν(C−O) frequency of functional kinase FixL-CO, relative to truncated FixL-CO, reflects a change in the geometry of the bound CO caused by increased steric constraint in the distal pocket imposed by the presence of the kinase domain (*28*). This explanation is favored over the alternative hypothesis that an electrostatic perturbation of the distal environment causes the observed frequency shift. The steric view is supported by EXAFS measurements showing a decrease in the Fe−C−O angle from 171° in truncated FixL-CO to 157° in functional kinase FixL-CO (*28*). The more linear CO coordination by truncated FixL-CO is thought to result in a more efficient overlap of CO and porphyrin π^* orbitals, leading to enhanced back-bonding and, consequently, higher ν(Fe−CO) and lower ν(C−O) frequencies than are observed in the functional kinase FixL-CO (*28*).

The DevS system is different from FixL in several respects: (1) both conformations of GAF A DevS-NO are six-coordinate complexes observable at room temperature, (2) the two distinct CO conformers observed in GAF A DevS are observed simultaneously rather than in different constructs as in FixL, and (3) the 35 cm^{-1} difference between the two ν(C−O) frequencies observed in GAF A DevS is more than 5-fold greater than the 6-cm^{-1} difference in ν(C−O) frequencies observed in truncated and functional kinase FixL. It seems unlikely that steric factors alone could account for such a significant difference in ν(C−O) frequencies in DevS. RR characterization of the CO adducts of a variety of myoglobin mutants shows that mutations affecting only steric crowding in the distal pocket have relatively little effect on Fe−C−O vibrational frequencies when compared to those which alter the electrostatic environment of the bound CO (*16*). Therefore, we favor a model where the two conformations of CO and NO observed in GAF A differ by the hydrogen bond interactions these groups engage in the distal pocket, and only occur to any significant extent in the absence of interdomain interactions.

In contrast to the carbonyl and nitrosyl complexes, oxygen binding in DevS seems impervious to the effects of truncation, yielding the same ν(Fe−O_2) at 563 cm^{-1} for all constructs. This frequency is low among heme proteins with neutral proximal histidines but compares well with those of other proposed O_2-sensors such as *Bs*HemAT (560 cm^{-1}) (*29*) and *Ec*DosH (562 cm^{-1}) (*30*) (Table 2). In these systems, the low ν(Fe−O_2) is thought to arise from the presence of a specific hydrogen bond to the bound O_2 (*29, 31*). Indeed, the crystal structure of O_2-bound *Ec*DosH reveals two hydrogen bond interactions between the guanidinium group of an arginine residue and bound oxygen, one to each atom of the oxy group at 2.70 and 2.94 Å (*31*). In the case of HemAT, RR characterization of a T95A variant (ν(Fe−O_2) = 569 cm^{-1}) confirmed that this threonine residue is critical for the low frequency of the ν(Fe−O_2) and led to the suggestion that it forms a hydrogen bond to bound O_2 (*32*). The absence of a crystal structure for DevS precludes the identification of a potential hydrogen bond donor in this protein, but the unusually low ν(Fe−O_2) and the sensitivity of this mode to H/D exchange strongly suggest that the O_2 group is engaged in a strong hydrogen bond interaction in the distal pocket of DevS.

The similarities in exogenous ligand vibration modes in full-length DevS and HemAT extend to the CO- and NO-complexes, as the Fe−C−O and Fe−N−O frequencies of these proteins are quite similar, and consistent with these ligands residing in a purely hydrophobic environment (Table 2). Therefore, it seems likely that specific hydrogen-bonding networks are responsible for selective oxygen sensing in these proteins, as has been suggested for HemAT (*29, 32, 33*). This view is supported by the apparent immunity of the ν(Fe−O_2) frequency of DevS to truncation, suggesting that the distal pocket of this protein is optimized to interact with oxygen and does so even when conformational rigidity is not imposed by the presence of the GAF B domain.

Based on the evidence acquired on the full-length and truncated constructs of DevS, we propose a model for ligand discrimination and signal transduction based on electrostatic interactions in the heme distal pocket of the GAF A domain. Oxygen bound to the heme is engaged in a direct hydrogen bond to a protein residue in the distal pocket. The kinase domain is expected to be inactive in this conformation based on the putative function of DevS, although direct evidence linking heme ligation state with kinase activity is currently lacking. Dissociation of O_2 from the heme under hypoxic conditions and/or displacement by NO disrupts this hydrogen bond network. The accompanying structural change at the

heme domain is communicated to the kinase domains via the GAF B domain, leading to kinase activity and induction of the dormancy regulon. This model is consistent with the observation that hypoxia and NO each lead to induction of the dormancy regulon and that O_2 competitively inhibits NO-mediated induction (*6*). The presence of the GAF B domain is essential in restricting the structure of the GAF A domain so that only the O_2 complex can stabilize the hydrogen bond network which presumably propagates to the kinase domain, modulating its activity. In this view, it is tempting to propose that the GAF B domain acts as a transducer in the sensory process and is also crucial to the discriminatory power of the GAF A domain. According to this model, CO-bound DevS would also be active, but the response of MTB to CO has not yet been investigated. Further studies linking heme ligation state to kinase activity will be necessary to test this model and are underway in our laboratories.

SUMMARY

DevS is a heme-based sensor protein kinase that mediates the response of MTB to hypoxia and nitric oxide. The truncated heme domain, GAF A DevS, displays significant conformational flexibility in the distal pocket as evidenced by the presence of two distinct conformations of CO and NO bound to this construct. Based on the observed ν(Fe−XO) and ν(X−O) (X = C or N), these conformations differ by the presence or absence of hydrogen bond interaction at the exogenous ligand group. Full-length DevS, FL DevS, preferentially stabilizes the CO and NO conformer lacking the hydrogen bond by restricting distal pocket flexibility via interaction between the GAF A and GAF B domains. These interactions may represent a pathway by which conformational changes at the GAF A domain are communicated to the kinase domain, thereby modulating its activity. In contrast to CO and NO, O_2 bound to these proteins invariably engages strong hydrogen bond interaction(s) in the distal pocket. Thus, signal transduction in DevS appears to be mediated by a specific hydrogen bond network that only O_2 can fully stabilize.

SUPPORTING INFORMATION AVAILABLE

UV−vis spectra of ferric and ferrous DevS constructs, low-frequency RR spectra of DevS−CO complexes, ν(C−O) versus ν(Fe−CO) correlation plots of heme protein−CO complexes, RR spectra of the three constructs ^{14}NO, ^{15}NO, and $^{15}N^{18}O$ complexes, $^{16}O_2$ minus $^{18}O_2$ difference spectra of GAF A and FL DevS−O_2 complexes in H_2O and D_2O. This material is available free of charge via the Internet at http://pubs.acs.org.

NOTE ADDED IN PROOF

Results of autophosphorylation assay for different heme ligation states of DevS have now been reported *(38)*.

REFERENCES

1. World Health Organization (2007) Fact sheet on TB, http://www.who.int/3by5/TBfactsheet.pdf.
2. Dick, T. (2001) Dormant tubercle bacilli: the key to more effective TB chemotherapy?, *J. Antimicrob. Chemother. 47*, 117−118.
3. Wayne, L. G., and Hayes, L. G. (1996) An in vitro model for sequential study of shiftdown of *Mycobacterium tuberculosis* through two stages of nonreplicating persistence, *Infect. Immun. 64*, 2062−2069.
4. Sherman, D. R., Voskuil, M., Schnappinger, D., Liao, R., Harrell, M. I., and Schoolnik, G. K. (2001) Regulation of the *Mycobacterium tuberculosis* hypoxic response gene encoding alpha-crystallin, *Proc. Natl. Acad. Sci. U.S.A. 98*, 7534−7539.
5. Cunningham, A. F., and Spreadbury, C. L. (1998) Mycobacterial stationary phase induced by low oxygen tension: Cell wall thickening and localization of the 16-kilodalton -crystallin homolog, *J. Bacteriol. 180*, 801−808.
6. Voskuil, M. I., Schnappinger, D., Visconti, K. C., Harrell, M. I., Dolganov, G. M., Sherman, D. R., and Schoolnik, G. K. (2003) Inhibition of respiration by nitric oxide induces a Mycobacterium tuberculosis dormancy program, *J. Exp. Med. 198*, 705−713.
7. Wayne, L. G., and Sohaskey, C. D. (2001) Nonreplicating persistence of *Mycobacterium tuberculosis*, *Annu. Rev. Microbiol. 55*, 139−163.
8. Choi, H. S., Rai, P. R., Chu, H. W., Cool, C., and Chan, E. D. (2002) Analysis of nitric oxide synthase and nitrotyrosine expression in human pulmonary tuberculosis, *Am. J. Respir. Crit. Care Med. 166*, 178−186.
9. Dasgupta, N., Kapur, V., Singh, K. K., Das, T. K., Sachdeva, S., Jyothisri, K., and Tyagi, J. S. (2000) Characterization of a two-component system, DevR-DevS, of *Mycobacterium tuberculosis*, *Tubercle Lung Dis. 80*, 141−159.
10. Roberts, D. M., Liao, R. P., Wisedchaisri, G., Hol, W. G., and Sherman, D. R. (2004) Two sensor kinases contribute to the hypoxic response of *Mycobacterium tuberculosis*, *J. Biol. Chem. 279*, 23082−23087.
11. Sardiwal, S., Kendall, S. L., Movahedzadeh, F., Rison, S. C., Stoker, N. G., and Djordjevic, S. (2005) A GAF domain in the hypoxia/NO-inducible *Mycobacterium tuberculosis* DosS protein binds haem, *J. Mol. Biol. 353*, 929−936.
12. Ioanoviciu, A., Yukl, E. T., Moënne-Loccoz, P., and Ortiz de Montellano, P. R. (2007) DevS, a heme-containing two-component oxygen sensor of *Mycobacterium tuberculosis*, *Biochemistry 46*, 4250−4260.
13. Spiro, T. G., and Li, X. Y. (1988) *Biological applications of Raman spectroscopy. Vol. 3. Resonance Raman spectra of hemes and metalloproteins* (Spiro, T. G., Ed.) pp 1−37, John Wiley & Sons, New York.
14. Hu, S., Smith, K. M., and Spiro, T. G. (1996) Assignment of protoheme resonance Raman spectrum by heme labeling in myoglobin, *J. Am. Chem. Soc. 118*, 12638−12646.
15. Ray, G. B., Li, X.-Y., Ibers, J. A., Sessler, J. L., and Spiro, T. G. (1994) How far can proteins bend the FeCO unit? Distal polar and steric effects in heme proteins and models, *J. Am. Chem. Soc. 116*, 162−176.
16. Li, T., Quillin, M. L., Phillips, G. N., Jr., and Olson, J. S. (1994) Structural determinants of the stretching frequency of CO bound to myoglobin, *Biochemistry 33*, 1433−1446.
17. Anderton, C. L., Hester, R. E., and Moore, J. N. (1997) A chemometric analysis of the resonance Raman spectra of mutant carbonmonoxy-myoglobins reveals the effects of polarity, *Biochim. Biophys. Acta 1338*, 107−120.
18. Ling, J., Li, T., Olson, J. S., and Bocian, D. F. (1994) Identification of the iron-carbonyl stretch in distal histidine mutants of carbonmonoxymyoglobin, *Biochim. Biophys. Acta 1188*, 417−421.
19. Tomita, T., Hirota, S., Ogura, T., Olson, J. S., and Kitagawa, T. (1999) Resonance Raman investigation of Fe-N-O structure of nitrosylheme in myoglobin and its mutants, *J. Phys. Chem. B 103*, 7044−7054.
20. Coyle, C. M., Vogel, K. M., Rush, T. S., 3rd, Kozlowski, P. M., Williams, R., Spiro, T. G., Dou, Y., Ikeda-Saito, M., Olson, J. S., and Zgierski, M. Z. (2003) FeNO structure in distal pocket mutants of myoglobin based on resonance Raman spectroscopy, *Biochemistry 42*, 4896−4903.
21. Hu, S., and Kincaid, J. R. (1991) Resonance Raman spectra of the nitric oxide adducts of ferrous cytochrome P450cam in the presence of various substrates, *J. Am. Chem. Soc. 113*, 9760−9766.
22. Vogel, K. M., Kozlowski, P. M., Zgierski, M. Z., and Spiro, T. G. (1999) Determinants of the FeXO (X = C, N, O) vibrational frequencies in heme adducts from experiment and density functional theory, *J. Am. Chem. Soc. 121*, 9915−9921.
23. Takahashi, S., Ishikawa, K., Takeuchi, N., Ikeda-Saito, M., Yoshida, T., and Rousseau, D. L. (1995) Oxygen-bound heme-heme oxygenase complex−Evidence for a highly bent structure of the coordinated oxygen, *J. Am. Chem. Soc. 117*, 6002−6006.

24. Unno, M., Matsui, T., Chu, G. C., Couture, M., Yoshida, T., Rousseau, D. L., Olson, J. S., and Ikeda-Saito, M. (2004) Crystal structure of the dioxygen-bound heme oxygenase from *Corynebacterium diphtheriae*: implications for heme oxygenase function, *J. Biol. Chem. 279*, 21055−21061.
25. Couture, M., Yeh, S. R., Wittenberg, B. A., Wittenberg, J. B., Ouellet, Y., Rousseau, D. L., and Guertin, M. (1999) A cooperative oxygen-binding hemoglobin from *Mycobacterium tuberculosis*, *Proc. Natl. Acad. Sci. U.S.A. 96*, 11223−11228.
26. Das, T. K., Weber, R. E., Dewilde, S., Wittenberg, J. B., Wittenberg, B. A., Yamauchi, K., Van Hauwaert, M. L., Moens, L., and Rousseau, D. L. (2000) Ligand binding in the ferric and ferrous states of *Paramecium* hemoglobin, *Biochemistry 39*, 14330−14340.
27. Lukat-Rodgers, G. S., and Rodgers, K. R. (1997) Characterization of ferrous FixL-nitric oxide adducts by resonance Raman spectroscopy, *Biochemistry 36*, 4178−4187.
28. Miyatake, H., Mukai, M., Adachi, S., Nakamura, H., Tamura, K., Iizuka, T., Shiro, Y., Strange, R. W., and Hasnain, S. S. (1999) Iron coordination structures of oxygen sensor FixL characterized by Fe K-edge extended x-ray absorption fine structure and resonance Raman spectroscopy, *J. Biol. Chem. 274*, 23176−23184.
29. Aono, S., Kato, T., Matsuki, M., Nakajima, H., Ohta, T., Uchida, T., and Kitagawa, T. (2002) Resonance Raman and ligand binding studies of the oxygen-sensing signal transducer protein HemAT from *Bacillus subtilis*, *J. Biol. Chem. 277*, 13528−13538.
30. Tomita, T., Gonzalez, G., Chang, A. L., Ikeda-Saito, M., and Gilles-Gonzalez, M. A. (2002) A comparative resonance Raman analysis of heme-binding PAS domains: heme iron coordination structures of the BjFixL, AxPDEA1, EcDos, and MtDos proteins, *Biochemistry 41*, 4819−4826.
31. Park, H., Suquet, C., Satterlee, J. D., and Kang, C. (2004) Insights into signal transduction involving PAS domain oxygen-sensing heme proteins from the X-ray crystal structure of *Escherichia coli* Dos heme domain (Ec DosH), *Biochemistry 43*, 2738−2746.
32. Ohta, T., Yoshimura, H., Yoshioka, S., Aono, S., and Kitagawa, T. (2004) Oxygen-sensing mechanism of HemAT from *Bacillus subtilis*: a resonance Raman spectroscopic study, *J. Am. Chem. Soc. 126*, 15000−15001.
33. Yoshimura, H., Yoshioka, S., Kobayashi, K., Ohta, T., Uchida, T., Kubo, M., Kitagawa, T., and Aono, S. (2006) Specific hydrogen-bonding networks responsible for selective O2 sensing of the oxygen sensor protein HemAT from *Bacillus subtilis*, *Biochemistry 45*, 8301−8307.
34. Tamura, K., Nakamura, H., Tanaka, Y., Oue, S., Tsukamoto, K., Nomura, M., Tsuchiya, T., Adachi, S., Takahashi, S., Iizuka, T., and Shiro, Y. (1996) Nature of endogenous ligand binding to heme iron in oxygen sensor FixL, *J. Am. Chem. Soc. 118*, 9434−9435.
35. Tsubaki, M., Srivastava, R. B., and Yu, N. T. (1982) Resonance Raman investigation of carbon monoxide bonding in (carbon monoxy)hemoglobin and -myoglobin: detection of Fe-CO stretching and Fe-C-O bending vibrations and influence of the quaternary structure change, *Biochemistry 21*, 1132−1140.
36. Van Wart, H. E., and Zimmer, J. (1985) Resonance Raman evidence for the activation of dioxygen in horseradish oxyperoxidase, *J. Biol. Chem. 260*, 8372−8377.
37. Letunic, I., Goodstadt, L., Dickens, N. J., Doerks, T., Schultz, J., Mott, R., Ciccarelli, F., Copley, R. R., Ponting, C. P., and Bork, P. (2002) Recent improvements to the SMART domain-based sequence annotation resource, *Nucleic Acids Res. 30*, 242−244.
38. Sousa, E. H. S., Tuckerman, J. R., Gonzalez, G., and Gilles-Gonzalez, M.-A. (2007) DosT and DevS are oxygen-switched kinases in *Mycobacterium tuberculosis*, *Protein Sci. 16*, in press.

BI7008695